ISSN: 2754-4753

Journal of Physics & Optics Sciences

SCIENTIFIC Research and Community

Research Article

Open Access

A Simple Approach to Determine Diffusion Coefficient of Salt in Various Foods

Pok Yuen Wong[1], Chi Fui Ni[2], Chenyu Chou[2], Shengkai Wang[2], Yujia Wang[1], Lisa R Wang[2] and Jian Jim Wang[3]*

[1]Phillips Academy Andover, 180 Main Street, Andover, MA 01810, USA

[2]The Pennington School, 112 W Delaware Ave, Pennington, NJ 08534, USA

[3]NanoNuvo Corporation, Belle Mead, New Jersey 08502, USA

ABSTRACT

This study presents a simple, low-cost methodology to experimentally determine salt diffusion coefficients in food matrices, demonstrated using five food types: potato, sweet potato, pumpkin, taro, and radish. Each sample was manually shaped into a sphere of known diameter and immersed in pre-mixed salt solutions. The salt concentration at the center of each sample was measured using a compact salt meter (LAQUAtwin-salt-11 by Horiba), and the data were fitted to a theoretical diffusion model to extract diffusion coefficients. The coefficients ranged from 6.0×10^{-10} m²/s in taro to 1.3×10^{-9} m²/s in pumpkin. The method was validated through simulation and titration, both showing strong agreement with experimental data and deviations under 10%. This approach stresses the simplicity, speed, and cost-effectiveness of the method in contrast to traditional techniques such as NMR and titration. Additionally, temperature effects were investigated, with experiments at 100°C yielding an activation energy of approximately 74 meV (7.13 kJ/mol). By successfully applying this method across diverse food types, this work offers a scalable and practical alternative for food processing, quality control, and educational purposes.

***Corresponding author**

Jian Jim Wang, NanoNuvo Corporation, Belle Mead, New Jersey 08502, USA.

Received: July 10, 2025; **Accepted:** July 15, 2025; **Published:** July 23, 2025

Keywords: Diffusion Coefficient, Salt Diffusion, Activation Energy, Food Matrix, Compact Salt Meter

Introduction

The diffusion coefficient is a fundamental parameter in the mass transfer equation, $\nabla \cdot \nabla T = 1/D\ \partial T/\partial t$, which describes the critical physical phenomenon of mass transfer and exchange [1,2]. As a key material property, it plays a vital role in characterizing materials and understanding their applications. Consequently, the development of accurate, efficient, and cost-effective methods for measuring diffusion coefficients has garnered significant interest [3-8].

Salt, or sodium chloride, is a crucial component in food science, significantly influencing food processing and storage applications [9-17]. Understanding the salt diffusion process is essential for optimizing these applications, as it directly impacts product quality, safety, and preservation. Accurate determination of the salt diffusion coefficient requires precise measurements of salt concentration and distribution, and various experimental methods have been employed to achieve this [4-7].

One established method for measuring salt distribution and concentration is Nuclear Magnetic Resonance (NMR) imaging [4,5]. Widely applied in chemistry and medicine, NMR imaging enables the identification and quantification of specific elements from the periodic table.

Another widely adopted approach is titration, a conventional technique for determining salt concentration [3,10]. Titration involves using silver nitrate as a reagent to precipitate chloride ions, allowing for the determination of chloride content. This value is then used to calculate the concentrations of sodium chloride (NaCl) and sodium (Na). Despite its reliability, titration requires skilled operators and specific equipment, such as silver electrodes and automatic titrators. Near Infrared spectroscopy (NIR) has also been employed in previous studies to determine salt concentration and distribution [6,7]. However, all of these techniques often involve expensive instrumentation or complex procedures [3-7].

We conducted a comprehensive review of existing research on measuring and estimating mass diffusion coefficients [16-30]. A review of existing literature reveals that salt diffusion coefficients in food matrices typically range from 10^{-11} to 10^{-9} m²/s, depending on temperature, matrix structure, and salt concentration. These values vary significantly across meat, vegetable, and dairy products. A detailed summary of representative diffusion coefficients reported in previous studies is provided in the Supplementary Materials.

Increasing the temperature from room temperature to 100°C typically raises the diffusion coefficient by approximately a factor of 10 [28,30]. This temperature dependence can be expressed using an Arrhenius-type equation, with activation energy serving as the key parameter governing the effect of temperature on diffusion. For example, the activation energy for salt diffusion in Chinese cabbages was approximately 66 kJ/mol [20].

Salt diffusion is a fundamental phenomenon critical to food processing and preservation. The diffusion coefficient is a vital parameter for modeling salt migration in food matrices. Traditional measurement techniques such as NMR imaging, titration, and NIR spectroscopy, while well-established, often involve high costs and complex protocols. This study introduces a cost-effective, straightforward alternative that retains high accuracy while eliminating these limitations [31].

The five food types studied-potato, sweet potato, pumpkin, taro, and radish-were chosen to represent a diverse set of food matrices with different moisture content, porosity, and fiber structure. These are commonly encountered in both food processing and household culinary settings.

Understanding diffusion behavior in such matrices has practical implications in food technology, including pickling, marination, and salt penetration control, as well as in pharmaceutical applications where plant-derived carriers are used for controlled solute delivery.

While our model assumes spherical symmetry and isotropic diffusion, which simplifies calculations and facilitates validation, it does not capture anisotropy in fiber direction or real-time concentration profiles due to destructive sampling. These limitations are acknowledged in our analysis and interpretation of the data.

This study aims to present and validate a simple, low-cost method for determining salt diffusion coefficients in various foods. The methodology relies on shaping food samples into spheres, measuring salt concentration at the center after soaking, and fitting the results to a theoretical diffusion model. The effectiveness of this approach is evaluated through experimental results, simulations, and comparisons with traditional titration methods and published literature.

Materials and Methods

Sample Preparation

Our research introduces a streamlined, cost-effective, and precise method for determining the salt diffusion coefficient in a range of food types. The food samples were cut into nearly perfect spherical shapes to ensure uniformity and facilitate theoretical and experimental analysis [31].

Specialized cutting tools and standard kitchen utensils, such as vegetable Y-peeler, were employed to achieve the desired geometry [32]. Foods like potato, sweet potato, pumpkin, taro, and radish require manual shaping [32]. Representative examples of these spherical samples, with varying radii, can be found in the Supplementary Materials.

The diameters of the prepared samples were measured using a digital caliper to ensure consistent dimensions. Multiple measurements were taken across different orientations, with deviations in diameter limited to less than 1 mm for all samples. These measurements were averaged to confirm the accuracy of the spherical geometry. Additionally, the samples' weights were recorded, and their densities calculated. Across at least 12 samples of the same food type, density variations remained within 4%, further validating the uniformity of the preparation process.

The rationale for using a spherical shape lies in its symmetry, which simplifies theoretical modeling and experimental measurement [32]. Spherical symmetry ensures that the distance from the center is the sole geometric parameter influencing diffusion, enabling direct comparisons between theoretical calculations and experimental results.

Prepared samples had radii ranging from 13 mm to 31 mm, with each sphere subjected to the experimental procedure detailed in subsequent sections. This preparation method allows the inclusion of diameter as an independent variable in the analysis, enhancing the robustness and applicability of the findings across various food types [32].

The study involved five types of food: potato, sweet potato, taro, radish, and pumpkin. Each sample was pre-cut and sculpted into spherical shapes with radii ranging from 13 mm to 31 mm. This controlled preparation facilitated consistent and reliable results by standardizing the diffusion surface area and geometry across all samples.

Experimental Setup

Brine Solution Preparation and Sample Submersion

The brine solution used in the experiment was uniformly prepared by dissolving high-purity (99.9%) sodium chloride (NaCl) into pure water to achieve a salt concentration of either 10% or 20% by weight. Multiple spherical food samples were submerged in the prepared solution for a predetermined period. To assess the salt concentration at the sample's core, each sample was retrieved after a recorded submersion time. Subsequently, the sample was cut to extract a small piece weighing approximately 1 mg from its center. This extracted piece was then analyzed to determine the salt concentration. While this measurement method is destructive, it offers the advantages of being simple, quick, cost-effective, and straightforward.

Measurement Tools and Procedure

To quantify the salt concentration, a compact salt meter (LAQUAtwin-salt-11 by Horiba) was utilized. This instrument allows precise and efficient measurement, ensuring accuracy by performing triplicate readings for each sample. The measurement process, from sample preparation to obtaining results, required less than 10 minutes per sample. This efficient approach ensured consistent and reliable data throughout the study.

The overall cost of the materials and tools used in the experiment totaled under $800, with the breakdown as follows:

- **Compact salt meter (LAQUAtwin-salt-11 by Horiba):** $180
- **200g x 0.1mg Digital Analytical Balance Lab Precision Scale (U.S. Solid):** $480
- **Caliper:** $20
- **Food materials (including salts):** $80
- **Containers, cookware, and other supplies:** $100

This economical setup ensured the feasibility of the research while maintaining high standards of measurement accuracy.

By enabling direct measurement from as little as a single drop of sample, the LAQUAtwin-salt-11 offers practicality and ease of use. It is capable of measuring absolute salt concentrations ranging from 0% to 15% with a relative precision of ±4%, ensuring reliable and accurate results during experimentation.

Sample Size and Experimental Validation

To ensure the reliability and accuracy of the measurements, repeated experiments were conducted using multiple batches of the same food sample type, all with identical diameters. Each experiment was repeated with 12 independent samples of the same food type to ensure reliability. The mean and standard deviation of salt concentrations were calculated for each set of samples. The measured salt concentration values from these repeated trials showed a variation within ±8%, affirming the robustness and repeatability of the method.

By employing a controlled brine solution, precise measurement tools, and a validated methodology, the study achieved consistent and reliable results, contributing valuable insights into salt diffusion in spherical food samples.

Validation Using Titration

To validate the salt concentration measurements, we conducted titration using silver nitrate as a reagent to precipitate chloride ions. This approach enabled us to calculate sodium chloride concentrations, which were subsequently compared with measurements obtained using the compact salt meter. A total of 12 standard samples were analyzed: 6 using the compact salt meter and 6 using the titration method.

The compact salt meter yielded measured results of (9.2 ± 0.3) × 10^{-10} m^2/s, while the titration method produced results of (9.3 ± 0.25) × 10^{-10} m^2/s. The results showed strong agreement between the two methods, with deviations of less than 5%, thereby confirming the reliability of the compact salt meter.

The Theoretical Model and Simulation

For the theoretical simulation, we consider a spherical model to approximate the system, assuming uniform salt diffusion from all directions. The sample begins with an initial salt concentration near zero and consists of a homogeneous material with known physical properties, such as its diameter. Salt concentration at the sphere's center is calculated and measured over time as a function of radius. The sample radius is a controlled variable, allowing comparisons across different samples.

The transport of molecules and ions, including salt, sugar, water, and oil, is governed by mass transfer, which can be described by Fick's Second Law. This equation is analogous to the heat transfer equation [32-34].

$$\nabla \cdot \nabla c = \frac{1}{D}\frac{\partial C}{\partial t} \qquad (1)$$

Here, C = C (x, t) represents the concentration of the molecules or ions, which is a function of both position and time. D is the diffusion coefficient of the molecules or ions, expressed in m^2/s.

For a sphere with azimuthal symmetry, during the mass transfer, we have $\frac{\partial C}{\partial \theta} = 0$ and $\frac{\partial^2 C}{\partial \varphi^2} = 0$. For brining (soaking) food with food starting with low concentration C0 and surrounded at high concentration (bath concentration) Ch, we have the following boundary conditions:

$C(r,o) = C_0$ $(0 \le r \le R)$, where R is the radius of the sphere.

$$C(\ge R, t) = C_h$$

We then have:

$$C(r,t) = C_h - \frac{2R(C_h - C_0)}{\pi \cdot r}\sum_{n=1}^{\infty}\left[\frac{(-1)^{n+1}}{n}\sin\frac{n\pi r}{R}\cdot e^{-n^2 t/\tau}\right] \quad (2)$$

for $(0 \le r \le R)$

We define

$$\tau = \frac{R^2}{\pi^2 \cdot D}$$ as the time constant.

Thus, we have:

$$C_c = C_h - 2(C_h - C_0)\sum_{n=1}^{\infty}\left[(-1)^{n+1}\cdot e^{-n^2 t/\tau}\right] \quad (3)$$

The concentration at the center of the sphere is (r = 0):

$$C(r,t) = C_h - \frac{2R(C_h - C_0)}{\pi \cdot r}\sum_{n=1}^{\infty}\left[\frac{(-1)^{n+1}}{n}\sin\frac{n\pi r}{R}\cdot e^{-Dn^2\pi^2 t/R^2}\right] \qquad (4)$$

We can spell out the equation with some of the initial (and deciding) terms:

$$C_c = C_h - 2(C_h - C_0)\left\{e^{-t/\tau} - e^{-4t/\tau} + e^{-9t/\tau} - e^{-16t/\tau} + e^{-25t/\tau} - e^{-36t/\tau} + e^{-49t/\tau} - \ldots\right\} \qquad (5)$$

Equation (5) is employed for all calculations involving the relationship between central ions concentration and time. In this equation, R represents the radius of each food sample measured using a caliper, and D denotes the mass diffusion coefficient for the ions (i.e., salt). The mass diffusion coefficient (D) serves as a fitting parameter for all the simulation fittings.

Experimental and Simulation Results

Figure 1 presents the measured center salt concentration (dots) for three potato samples with identical radii as a function of time. The data reveals that the center salt concentration increases with longer brining durations. The solid curves in the figure represent theoretical simulation results using three different salt diffusion coefficients: 10^{-10} m^2/s, $1x10^{-10}$ m^2/s, and $1.2x10^{-9}$ m^2/s, respectively. Among these, the curve with a diffusion coefficient of $1x10^{-9}$ m^2/s aligns closely with the experimental data.

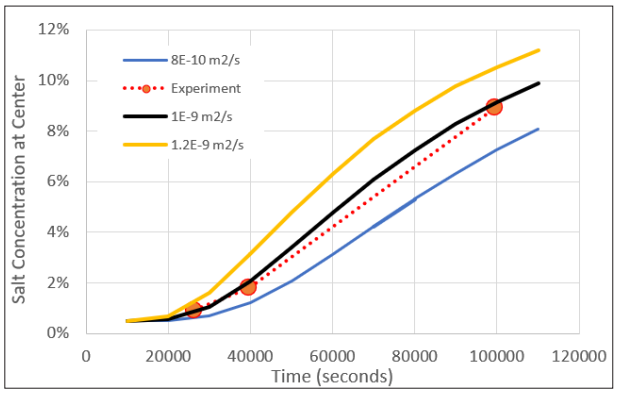

Figure 1: Potato Samples with a Uniform Radius of 24 mm were Measured. The Center Salt Concentration of the Spherical Samples was Recorded as a Function of Brine time, Represented by Dots. The Solid Curves Correspond to Simulation Results, with the Diffusion Coefficient being the only Variable.

Figure 2 illustrates the center salt concentration measurements (dots) for two potato samples with radii of 24 mm and 28.5 mm, respectively, after being brined for an identical duration of 24 hours (86,400 seconds). The solid curves depict theoretical simulation results using three different salt diffusion coefficients: 8x10-10 m^2/s, $1x10^{-9}$ m^2/s, and $1.2x10^{-9}$ m^2/s, respectively. Among these, the simulation curve with a diffusion coefficient of $1x10^{-9}$ m^2/s aligns most closely with the experimental data.

Figure 3 shows the center salt concentration measurement results (dots) for five potato samples with varying radii of 13 mm, 18 mm, 21.5 mm, 27 mm, and 31 mm. All samples were brined for an identical duration of 24 hours (86,400 seconds). The solid curves represent theoretical simulation results using three different salt diffusion coefficients: $6x10^{-10}$ m^2/s, $9x10^{-10}$ m^2/s, and $1x10^{-9}$ m^2/s, respectively.

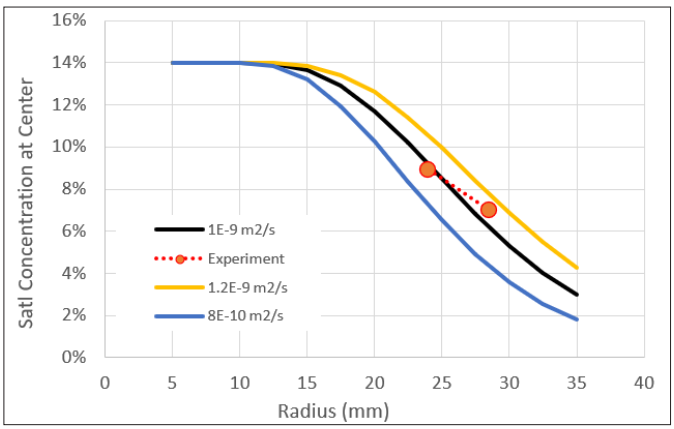

Figure 2: Center Salt Concentration Measurement Results (dots) for two Potato Samples with Radii of 24 mm and 28.5 mm, respectively. The Brine time Duration is Fixed at 24 Hours (86,400 Seconds). The Dots Represent the Recorded Salt Concentration at the center of the spherical samples as a function of radius. The solid curves correspond to simulation results, with the diffusion coefficient as the only variable.

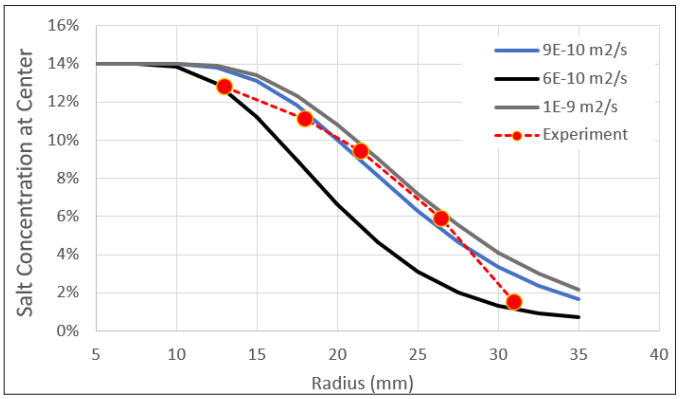

Figure 3: Center salt concentration measurement results (dots) for five sweet potato samples with radii of 13 mm, 18 mm, 21.5 mm, 27 mm, and 31 mm. The brine time duration is fixed at 24 hours (86,400 seconds). The dots represent the recorded salt concentration at the center of the spherical samples as a function of radius. The solid curves correspond to simulation results, with the diffusion coefficient as the only variable.

Figure 4 presents the center salt concentration measurement results (dots) for two taro samples with radii of 21 mm and 24.5 mm, respectively. Both samples were brined for the same duration of 24 hours (86,400 seconds). The solid curves represent theoretical simulation results with salt diffusion coefficients of $6x10^{-10}$ m^2/s, $7.5x10^{-10}$ m^2/s, and $9x10^{-10}$ m^2/s, respectively. Among these, the curve with a diffusion coefficient of $7x10^{-10}$ m^2/s aligns closely with the experimental data.

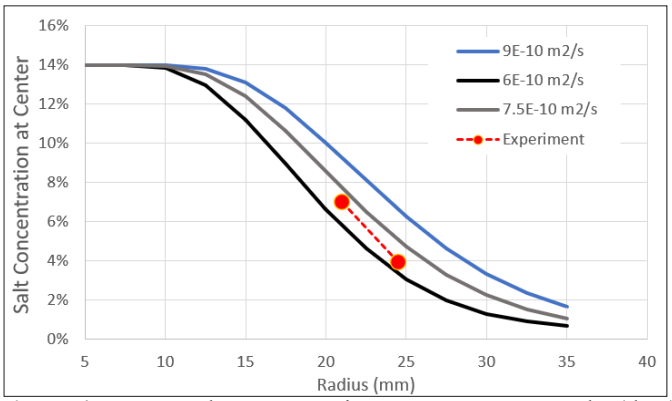

Figure 4: Center Salt Concentration Measurement Results (dots) for two Taro Samples with Radii of 21 mm and 24.5 mm. The Brine Time Duration is fixed at 24 Hours (86,400 Seconds). The Dots Represent the Recorded Salt Concentration at the Center of the Spherical Samples as a Function of Radius. The Solid Curves Correspond to Simulation Results, with the Diffusion Coefficient as the only Variable.

Figure 5 presents the center salt concentration measurement results (dots) for two radish samples with radii of 19 mm and 25.5 mm, respectively. Both samples were brined for the same duration of 24 hours (86,400 seconds). The solid curves represent theoretical simulation results with salt diffusion coefficients of $6x10^{-10}$ m^2/s, $7.5x10^{-10}$ m^2/s, and $9x10^{-10}$ m^2/s, respectively. Among these, the curve with a diffusion coefficient of $7.5x10^{-10}$ m^2/s shows the best agreement with the experimental data.

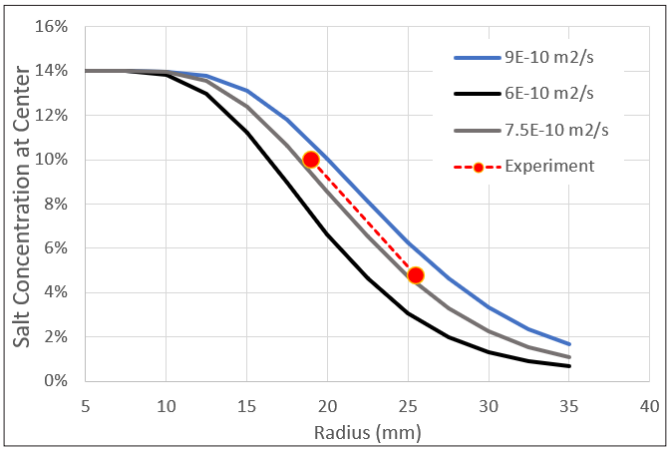

Figure 5: Center Salt Concentration Measurement Results (dots) for two Radish Samples with radii of 19 mm and 25.5 mm. The Brine time Duration is fixed at 24 Hours (86,400 Seconds). The dots represent the recorded salt concentration at the center of the spherical samples as a function of radius. The solid curves correspond to simulation results, with the diffusion coefficient as the only variable.

In this research, the temperature dependency of diffusion is also investigated, described by the Arrhenius equation [28,30].

$$D_e = D_0 e^{-\frac{E_a}{RT}}$$

Where De is the effective diffusion coefficient in m^2/s, Ea is the activation energy in meV or J/mol, D0 is the pre-exponential factor in m^2/s, R is the gas constant (8.314 J/mol K), and T is the absolute temperature.

To measure salt diffusion coefficients at different temperatures, the experimental setup and measurement method were adjusted accordingly.

Figure 6 presents the center salt concentration measurement results (dots) for two potato samples with radii of 24 mm and 26 mm, respectively. Unlike previous experiments conducted at room temperature, the brining process in this case was carried out at 100°C. The brine time duration for both samples was 3 hours (10,800 seconds). The solid curves represent theoretical simulation results with salt diffusion coefficients of $7x10^{-9}$ m^2/s, $8x10^{-9}$ m^2/s, and $1.1x10^{-8}$ m^2/s, respectively. The curve with a diffusion coefficient of $1x10^{-8}$ m^2/s aligns closely with the experimental data.

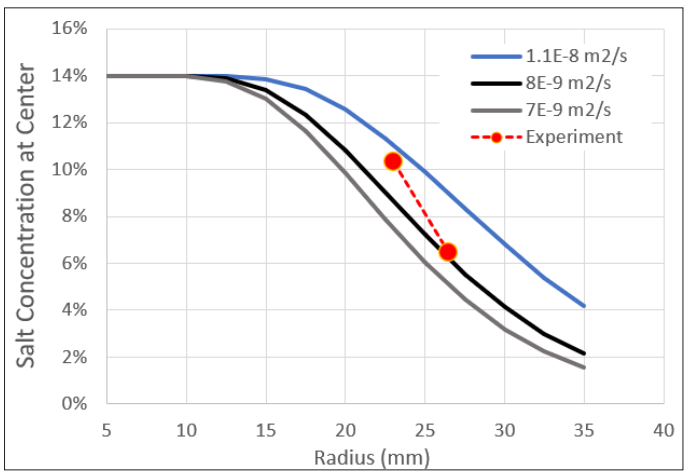

Figure 6: Center Salt Concentration Measurement Results (dots) for two Potato Samples with Radii of 24 mm and 26 mm, Measured at 100°C. The Brine time Duration is Fixed at 3 Hours (10,800 Seconds). The Dots Represent the Recorded Salt Concentration at the Center of the Spherical Samples as a Function of Radius. The Solid Curves Correspond to Simulation Results, with the Diffusion Coefficient as the only Variable.

For comparison, Figure 7 presents two sets of data: one obtained at room temperature and the other at 100°C. This comparison facilitates an assessment of the temperature's effect on the salt diffusion process, highlighting the differences in salt concentration measurements between the two temperatures. Analyzing these differences provides valuable insights into the role of temperature in salt diffusion and enables more accurate predictions of salt diffusion coefficients under varying thermal conditions.

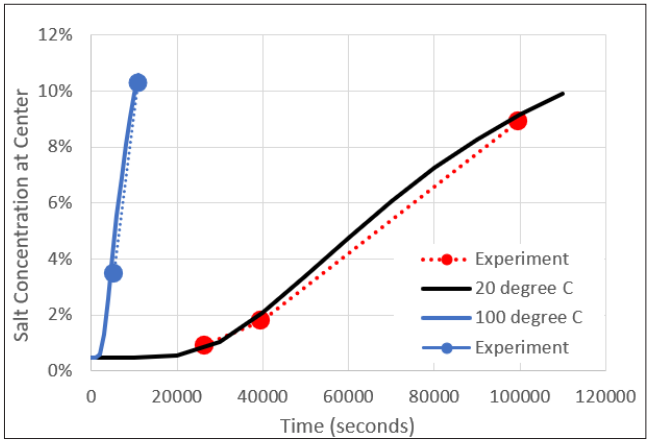

Figure 7: Center salt concentration measurement results (dots) for potato samples with a uniform radius of 24 mm, measured at two different temperatures: 20°C and 100°C. The dots represent the recorded salt concentration at the center of the spherical samples as a function of brine time. The solid curves correspond to simulation results, with the diffusion coefficient as the only variable.

Using the Arrhenius equation, $D_e = D_0 e^{-\frac{E_a}{RT}}$, we can derive the activation energy (Ea) for the salt diffusion process. In our study, with T = 373K and De ranging between $8x10^{-9}$ m^2/s to $1.1x10^{-8}$ m^2/s, and D0 ranging between $8x10^{-10}$ m^2/s to $1.2x10^{-9}$ m^2/s, we calculate the activation energy to be around 74meV or 7.13 kJ/mol. This value provides valuable insight into the temperature dependence of the salt diffusion process and can be utilized to predict diffusion rates under varying conditions.

Results and Discussion

Diffusion Coefficients Across Food Types

	Diffusion Coefficient (10^{-10} m^2/s) @ 20°C	
Food	**Low end value**	**High end value**
Potato	8.0	12.0
Pumpkin	11.0	13.0
Sweet potato	6.0	10.0
Taro	6.0	7.5
Radish	7.5	9.0

Table 1: Diffusion Coefficients of Salt in Five Food Types. This table presents the experimentally determined diffusion coefficients of salt for five distinct food types, measured at 20°C. Spherical samples were used, and the salt concentration at the center was recorded. Data were fitted to a theoretical model based on Fick's Law, with the diffusion coefficient serving as the primary fitting parameter, enabling accurate quantification of salt diffusivity in each food matrix.

Table 1 summarizes the diffusion coefficients of salt in five distinct food types, determined through experimental measurements and validated using theoretical simulations based on Fick's Law at 20°C. Spherical food samples were utilized to ensure uniformity and reproducibility of results. The observed diffusivity ranges highlight variations in structural and compositional properties across food types, such as moisture content, cellular density, and matrix porosity, which influence salt diffusion rates. These findings not only align with existing literature [16-30] but also underscore the precision of the proposed methodology in capturing solute transport dynamics in diverse food matrices.

- Potato exhibits diffusion coefficients ranging from 8.0×10^{-10} m^2/s to 12.0×10^{-10} m^2/s, demonstrating moderate diffusivity likely due to its dense structure.
- Sweet Potato shows slightly lower values, between 6.0×10^{-10} m^2/s and 10.0×10^{-10} m^2/s, consistent with its starch-rich composition.
- Pumpkin has the highest diffusivity, ranging from 11.0×10^{-10} m^2/s to 13.0×10^{-10} m^2/s, likely attributable to its high moisture content and porous structure.
- Taro and Radish demonstrate relatively lower diffusion coefficients of 6.0×10^{-10} to 7.5×10^{-10} m^2/s and 7.5×10^{-10} to 9.0×10^{-10} m^2/s, respectively, aligning with their denser cellular matrices.

These findings align with trends reported in existing literature, confirming the reliability of the measurement approach while also highlighting the reduced uncertainty achieved through the proposed method [16-30].

The diffusion coefficients were obtained with 95% confidence intervals. Error propagation analysis was conducted to evaluate the impact of deviations in sample diameter and salt concentration measurements on the final diffusion coefficients. The total error was estimated to be within ±12%.

Temperature Dependency

Diffusivity increased significantly when the temperature was raised from room temperature to 100°C. This behavior is consistent with the Arrhenius equation, where higher temperatures enhance molecular motion, facilitating diffusion. The calculated activation energy of 7.13 kJ/mol is consistent with published values, further validating the experimental results [16-20]. This temperature-dependent behavior underscores the importance of considering thermal effects when modeling or predicting diffusion in practical applications such as cooking or food preservation.

Simulation Validation

Theoretical modeling based on Fick's Law accurately predicted the salt concentration at the center of samples over time, with deviations below 10% across all tested food types. This strong agreement highlights the robustness of the simulation approach and its applicability for predicting diffusion in complex food matrices.

Discussion

Comparative Advantages of the Method

This study presents a novel approach for measuring salt diffusion coefficients in food, characterized by several advantages over traditional techniques:

- **Cost-Effectiveness:** The total experimental setup costs less than $800, significantly lower than NMR or titration setups.
- **Simplicity:** The method eliminates the need for complex instrumentation or specialized skills, making it accessible for small-scale labs and industry.
- **High Repeatability:** The method consistently produced reliable results with minimal variability across repeated measurements.
- **Alignment with Established Methods:** Strong agreement with results from titration and NMR imaging underscores the accuracy and reliability of the proposed approach.
- **Scalability:** The approach can be extended to other solutes and food matrices, broadening its applicability in food processing and preservation.

Compared to advanced methods such as Nuclear Magnetic Resonance (NMR) imaging and Near-Infrared (NIR) spectroscopy, our approach yields diffusion coefficient values that are consistent with those reported in the literature, while dramatically reducing experimental complexity and cost. For instance, Floury et al [27]. reported salt diffusivities in cheese matrices ranging from 1 to 5.5 × 10^{-10} m^2/s using NMR techniques, and Volpato et al [16]. found values of 8.99–9.55 × 10^{-10} m^2/s in chicken breast through time-consuming curing trials. Our measured ranges, such as 6.0–10.0 × 10^{-10} m^2/s for sweet potato and 11.0–13.0 × 10^{-10} m^2/s for pumpkin, are within or above these ranges and were obtained with under 10% deviation using a handheld meter and a simplified spherical diffusion model. This highlights not only the method's accuracy but also its accessibility, allowing similar-quality results without the need for high-end instrumentation or extended curing periods. Additionally, our method demonstrated strong agreement with silver nitrate titration and theoretical simulations, further validating its reliability across diverse food matrices.

Limitations

Despite its Advantages, the Method has Limitations:

- **Destructive Sampling:** The requirement for cutting and analyzing the sample precludes reuse.
- **Environmental Sensitivity:** Factors such as ambient humidity or non-uniform brine conditions can influence results.
- **Shape Dependency:** While shape deviations were accounted for using a shape factor, significant deviations from spherical geometry may introduce additional errors.
- **Implications for Industry**
- The findings have significant implications for food processing industries:
- **Applications:** The method can be applied in processes like pickling, salting, and blanching, where precise diffusivity measurements are critical for product quality and process optimization.
- **Customizability:** The approach is adaptable for studying other solutes and food types, broadening its industrial relevance.

Error Analysis

The calculated confidence intervals and error analysis suggest that the proposed method provides reliable diffusion coefficients with minimal variability. Sources of error, such as measurement inaccuracies and geometric deviations, were controlled through stringent sample preparation and measurement protocols. The variability across replicates was minimal, with standard deviations below ±10% of the mean, highlighting the repeatability of the measurements.

Salt Meter Precision

Variability due to meter sensitivity and sample placement could introduce minor inaccuracies. However, high repeatability across multiple trials mitigates this potential error.

Sample Geometry

Deviations from perfect spheres were evaluated using a shape factor, S [32, 33]. Analysis revealed that minor deviations had negligible impacts on final data accuracy, as verified by the consistency of results from samples with varying shapes.

Brine Conditions

Non-uniformities in brine during immersion could potentially affect diffusion rates. However, the controlled experimental setup minimized such variations, ensuring consistent conditions across trials.

Measurement of Radius

Errors in diameter measurement were minimized by cross-validating with mass measurements. This dual-check system enhanced overall accuracy.

Validation with Reference Methods

To validate the proposed method, diffusion coefficients were compared against results obtained through titration and NMR imaging. Strong agreement was observed, with deviations under 10%, demonstrating the reliability of the approach. The method's reduced complexity and cost make it an attractive alternative to more resource-intensive techniques without compromising accuracy.

Summary

This research experimentally determined the salt diffusion coefficients for five types of foods: potato, sweet potato, pumpkin, taro, and radish, using a simple, low-cost method. Spherical food samples with known diameters were immersed in a pre-mixed salt solution for specified soaking times. After soaking, a small piece was extracted from the center of each sample, and the salt concentration was measured using a compact salt meter (LAQUAtwin-salt-11) by Horiba.

Salt concentration measurements, taken as functions of diameter and soaking time, were compared with simulation results. By fitting the experimental data to the simulations, the diffusion coefficients for each food type were determined, showing strong agreement between measured and simulated values. Additionally, the salt diffusion coefficient for potato was measured at 100°C, enabling the calculation of an activation energy of approximately 74 meV (7.13 kJ/mol).

This study highlights a simple, cost-effective method for determining salt diffusion coefficients, validated against established techniques. The approach is scalable for industrial applications and provides a solid foundation for further research.

These comparisons underscore the methodological advantages of our technique in terms of affordability, speed, and suitability for rapid diffusivity screening in both academic and industrial settings.

Acknowledgments

The experiments in this research were conducted in a home kitchen "laboratory." The authors are deeply grateful to their parents for their unwavering support, both financial and moral, which made it possible to purchase the necessary tools and equipment. Special thanks go to The Pennington School and Phillips Academy Andover for providing resources and facilities that contributed to this study.

References

1. Bird RB, Stewart WE, Lightfoot EN (2006) Transport Phenomena (2nd ed). John Wiley & Sons 928.
2. Welti-Chanes J, Vergara-Balderas F, Bermu´dez-Aguirre D (2005) Transport phenomena in food engineering: basic concepts and advances. Journal of Food Engineering 67: 113-128.
3. Theodoros H Varzakas, Gareth C Leach, Cleanthes J Israilides, Dimitrios Arapoglou (2005) Theoretical and experimental

approaches towards the determination of solute effective diffusivities in foods. Enzyme and Microbial Technology 37: 29-41.

4. Hanne Christine Bertram, Samantha J Holdsworth, Andrew K Whittaker, Henrik J Andersen (2005) Salt Diffusion and Distribution in Meat Studied by 23 Na Nuclear Magnetic Resonance Imaging and Relaxometry. Journal of Agricultural and Food Chemistry 53: 7814-7818.
5. Emmanuel Hatzakis (2018) Nuclear Magnetic Resonance (NMR) Spectroscopy in Food Science: A Comprehensive Review. Comprehensive Reviews in Food Science and Food Safety 18: 189-220.
6. Ellekjær MR, Hildrum KI, Næs T, Isaksson T (1993) Determination of the Sodium Chloride Content of Sausages by near Infrared Spectroscopy. J Near Infrared Spectrosc 1: 65-75.
7. Laub Ekgreen MH, Martinez Lopez B, Jessen F, Skov T (2018) Non-destructive measurement of salt using NIR spectroscopy in the herring marinating process. Lebensmittel-Wissenschaft und Technologie 97: 610-616.
8. Daniel Caballero, Andrés Caro, Pablo G Rodríguez, María Luisa Durán, María del Mar Ávila, et al. (2016) Modeling salt diffusion in Iberian ham by applying MRI and data mining. Journal of Food Engineering 189: 115-122.
9. Huang E, Mittal GS (1995) Meatball cooking-modeling and simulation. Journal of Food Engineering 24: 87-100.
10. Ellen R Bornhorst, Juming Tang, Shyam S Sablani (2016) Sodium Chloride Diffusion in Low-Acid Foods during Thermal Processing and Storage. E1130 Journal of Food Science 81: 5.
11. Stapley GF, Fryer PJ, Gladden LF (1998) Diffusion and Reaction in Whole Wheat Grains during Boiling. AIChE Journal 44: 1778.
12. Ikuko Maeda, Akemi K Horigane, Mitsuru Yoshida, Yoshihiro Aikawa (2009) Water Diffusion in Buckwheat Noodles and Wheat Noodles during Boiling and Holding as Determined from MRI and Rectangular Cylinder Diffusion Model. Food Sci Technol Res 15: 107-116.
13. Jousse F, Agterof W, Jongen T, Koolschijn M, Visser A, et al. (2002) Flavor Release from Cooking Oil during Heating. Journal of food science 67: 2987-2996.
14. Minqi Wang, Takahiko Doi, David Julian McClements (2019) Encapsulation and controlled release of hydrophobic flavors using biopolymer-based microgel delivery systems: Sustained release of garlic flavor during simulated cooking. Food Research International 119: 6-14.
15. Danae Doulia, Tzia K, Gekas V (2000) A knowledge base for the apparent mass diffusion coefficient (DEFF) of foods. International Journal of Food Properties 3: 1-14.
16. Juliane Floury, Sophie Jeanson, Samar Aly, Sylvie Lortal (2010) Determination of the diffusion coefficients of small solutes in cheese: A review. Dairy Sci Technol 90: 477-508.
17. Volpato G, Michielin EMZ, Ferreira SRS, Petrus JCC (2007) Kinetics of the diffusion of sodium chloride in chicken breast (pectoralis major) during curing. Journal of Food Engineering 79: 779-785.
18. Hui Li, Cuiping Zhao, Yunhan Guo, Kejing An, Shenghua Ding, et al. (2012) Mass transfer evaluation of ultrasonic osmotic dehydration of cherry tomatoes in sucrose and salt solutions. International Journal of Food Science and Technology 47: 954-960.
19. Ahmet Akköse, Nesimi Aktaş (2016) Determination of Salt Diffusion Coefficient in Rainbow Trout (Oncorhynchusmykiss). Journal of Aquatic Food Product Technology 25: 344-349.
20. Cho HY, Kim JB, Pyun YR (1988) Diffusion of sodium chloride in Chinese cabbage during salting. Korean J Food Sci Technol 20: 711-717.
21. Graiver N, Pinotti A, Califano A, Zaritzky N (2006) Diffusion of sodium chloride in pork tissue. Journal of Food Engineering 77: 910-918.
22. Rodger G, Hastings R, Cryne C, Bailey J (1984) Diffusion Properties of Salt and Acetic Acid into Herring and Their Subsequent Effect on the Muscle Tissue. Journal of Food Science 49: 714-720.
23. Dihui Wang, Juming Tang, Lino RC (2000) Salt diffusivities and salt diffusion in farmed Atlantic salmon muscle as influenced by rigor mortis. Journal of Food Engineering 43: 115-123.
24. Clémentine Lauverjat, Clément de Loubens, Isabelle Déléris, Ioan Cristian Tréléa, Isabelle Souchon (2009) Rapid determination of partition and diffusion properties for salt and aroma compounds in complex food matrices. Journal of Food Engineering 93: 407-415.
25. Sabadini E, Carvalho BC, Sobral PJ do A, Hubinger MD (1998) Mass Transfer and Diffusion Coefficient Determination in the Wet and Dry Salting of Meat. Drying Technology: An International Journal. 16: 2095-2115.
26. Behrouz Mosayebi Dehkordi, Frazaneh Hashemi, Ramin Mostafazadeh (2010) Numerical Solution of the Equations of Salt Diffusion into the Potato Tissues. International Journal of Chemical and Biological Engineering 3: 2.
27. Floury J, Olivier R, Maëva LP, Marie HF (2009) Reducing salt level in food: Part 2: Modelling salt diffusion in model cheese systems with regards to their composition. LWT - Food Science and Technology 42: 1621-1628.
28. Gómez J, Sanjuán N, Bon J, Arnau J, Clemente G (2015) Effect of temperature on nitrite and water diffusion in pork meat. Journal of Food Engineering 149: 188-194.
29. Graiver N, Pinotti A, Califano A, Zaritzky N (2009) Mathematical modeling of the uptake of curing salts in pork meat. Journal of Food Engineering 95: 533-540.
30. Chitra Kusnadi, Sudhir K Sastry (2012) Effect of Temperature on Salt Diffusion into Vegetable Tissue. International Journal of Food Properties 15: 1148-1160.
31. Lisa R Wang, Yifei Jin, Songhe Shen, Liangxi Chen, William X Li, et al. (2023) A Simple Approach to Determine Diffusion Coefficient of Salt in Various Food. 2023 APS March Meeting 68. https://meetings.aps.org/Meeting/MAR23/SessionIndex2/?VirtualSession=T.
32. Lisa R Wang, Yifei Jin, Jian Jim Wang (2022) A Simple and Low-cost Experimental Method to Determine the Thermal Diffusivity of Various Types of Foods. American Journal of Physics 90: 568-572.
33. Yifei Jin, Lisa R Wang, Jian Jim Wang (2021) Physics in turkey cooking: Revisit the Panofsky formula. AIP Advances 11: 115316.
34. James RW, Charles EW, Robert EW, Gregory LR () Fundamentals of Momentum, Heat, and Mass Transfer, 5th Edition.

Supplemental Materials

A detailed summary of representative diffusion coefficients reported in previous studies is provided below:

Floury et al., for example, investigated NaCl diffusion in cheese using NMR and reported diffusion coefficients ranging from 1

to 5.5 × 10^{-10} m^2/s at 10–15°C. Similarly, the diffusivities of sodium chloride in chicken breast were found to range between 8.99 × 10^{-10} m^2/s and 9.55 × 10^{-10} m^2/s [17]. In beef, salt diffusion coefficients varied from 5 to 39 × 10^{-10} m^2/s [18], while salt and sugar diffusion in vegetables were reported to range from 2 to 30 × 10^{-10} m^2/s [30]. NaCl diffusion in Chinese cabbages was measured between 1.7 and 11.6 × 10^{-11} m^2/s [20].

The effective diffusion coefficient of NaCl (Dm) in pork tissue was reported to range from 0.6 to 5 × 10^{-10} m^2/s, depending on the brine NaCl concentration [21, 28–29]. In potato tissue, the diffusion coefficient was measured between 3.45 and 4.39 × 10^{-9} m^2/s [26]. Diffusion coefficients for chloride, nitrite, and nitrate in beef and pork ranged from 1 to 5 × 10^{-10} m^2/s, while salt diffusion in beef, salmon, and cheese was measured within 1 to 7 × 10^{-10} m^2/s. The diffusion of salt and acetic acid into herring ranged from 1 to 6 × 10^{-10} m^2/s [22]. For salted duck eggs, diffusion coefficients ranged from 2 × 10^{-10} m^2/s to 2 × 10^{-11} m^2/s. In dehydrated salted meat, the diffusion coefficient for wet salting was 0.26 × 10^{-10} m^2/s at 20°C and 0.25 × 10^{-10} m^2/s at 10°C, while for dry salting, it was significantly higher, at 19.37 × 10^{-10} m^2/s at 20°C and 17.21 × 10^{-10} m^2/s at 10°C [29].

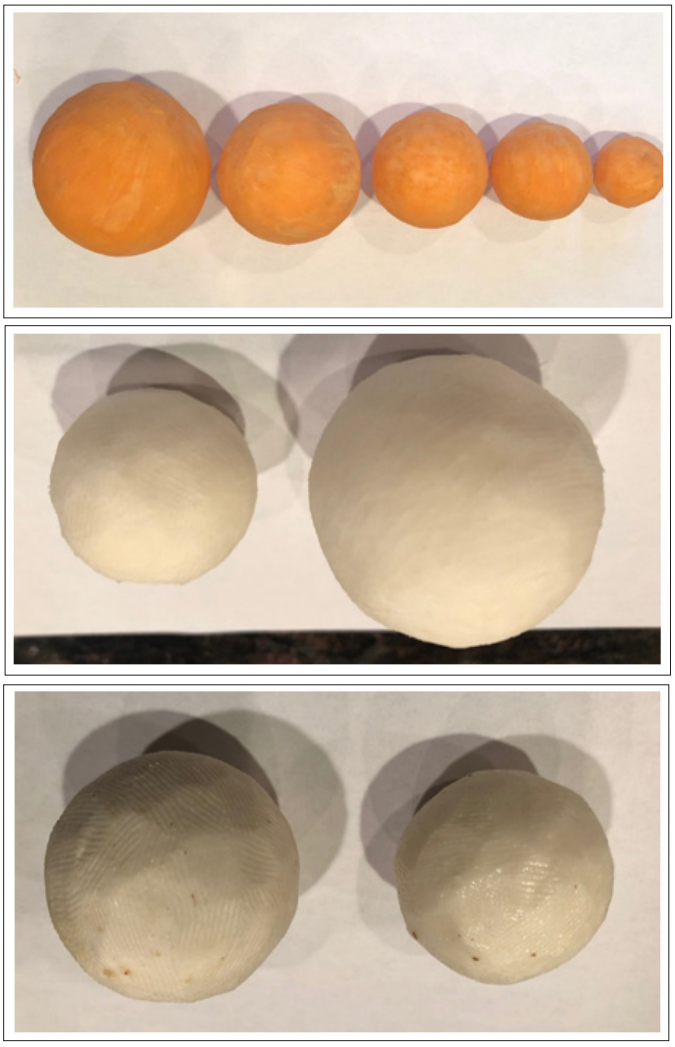

Figure S1: Representative spherical food samples (potato, sweet potato, taro, radish, and pumpkin) with radii ranging from 13 mm to 31 mm used for salt diffusion analysis.

Figure S1 showcases the representative food samples used in the study, which were carefully shaped into spheres with varying diameters to ensure uniform geometry for salt diffusion analysis.

Figure S2(a) schematically illustrates the theoretical model of salt diffusion in an ideal spherical sample with azimuthal symmetry. In this model, salt diffuses uniformly and symmetrically from the surface toward the center along the azimuthal axis, ensuring consistent gradients. Figure S2(b) depicts the experimental configuration designed to approximate this theoretical symmetry. In this setup, a sphere-shaped food sample is submerged in a brine solution (10% or 20% NaCl by weight) for a controlled period ranging from 1 to 24 hours. The spherical geometry and uniform immersion facilitate symmetrical diffusion, allowing experimental results to align with theoretical expectations.

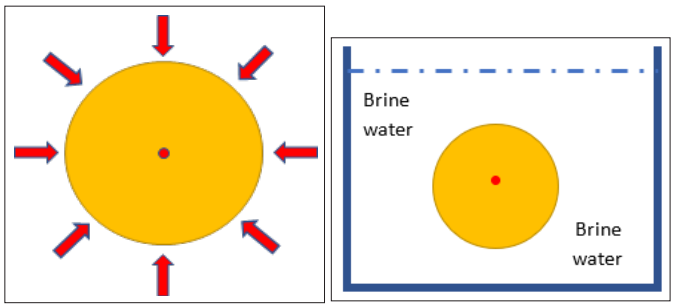

Fig. S2(a) Fig. S2(b)

Figure S2: (a) Theoretical model of salt diffusion with azimuthal symmetry in an ideal sphere. (b) Experimental setup showing a spherical food sample submerged in brine for 1–24 hours.

Figure S3 illustrates the compact salt meter, LAQUAtwin-salt-11 by Horiba, employed in this research to measure salt concentrations. This innovative device integrates the electrode, display, and sample container into a single compact unit, facilitating straightforward and efficient on-site testing.

Figure S3: The compact salt meter (LAQUAtwin-salt-11 by Horiba) used in this research. It measures salt concentrations (0%–15%) with a relative precision of ±4%, allowing direct measurement from a single drop.

Diffusion Equations and Mathematics

Fick's Law states [31, 32] that the mass transfer (i.e., diffusion) equation follows

$$\frac{\partial^2 C}{\partial x^2} = \frac{1}{D}\frac{\partial C}{\partial t}$$

Where C = C (x, t) and D is the mass diffusion coefficient in m^2/s. In three-dimension, the mass transfer equation becomes:

$$\nabla \cdot \nabla C = \frac{1}{D}\frac{\partial C}{\partial t}$$

Where,

$$\nabla \cdot \nabla T = \frac{\partial^2 C}{\partial x^2} + \frac{\partial^2 C}{\partial y^2} + \frac{\partial^2 C}{\partial z^2} \quad (for\ Cartisian\ coordinates)$$

$$= \frac{1}{r^2 \sin\theta}\left[\sin\theta \frac{\partial}{\partial r}\left(r^2 \frac{\partial C}{\partial r}\right) + \frac{\partial}{\partial \theta}\left(\sin\theta \frac{\partial C}{\partial \theta}\right) + \frac{1}{\sin\theta}\frac{\partial^2 C}{\partial \varphi^2}\right] \quad (for\ spherical\ coordinates)$$

$$= \frac{1}{r}\frac{\partial}{\partial r}\left(r\frac{\partial C}{\partial r}\right) + \frac{1}{r^2}\left(\frac{\partial^2 C}{\partial \theta^2}\right) + \frac{\partial^2 C}{\partial z^2} \quad (for\ cylinderical\ coordinates)$$

For a sphere with azimuthal symmetry, during the mass transfer, we have $\frac{\partial C}{\partial \theta} = 0$ and $\frac{\partial^2 C}{\partial \varphi^2} = 0$, the mass transfer equation becomes

$$\frac{1}{r^2}\left[\frac{\partial}{\partial r}\left(r^2 \frac{\partial C}{\partial r}\right)\right] = \frac{1}{D}\frac{\partial C}{\partial t}$$

Applying V = *r*·C to the above equation, for 0≤ r ≤ R we get:

$$\frac{\partial^2 V}{\partial r^2} = \frac{1}{D}\frac{\partial V}{\partial t}$$

We can decouple V(r, t) into:

$$V(r,t) = R(r)\cdot C(t)$$

And we get:

$$\frac{\partial V}{\partial t} = R(r)\cdot\frac{\partial C}{\partial t} = R(r)\cdot C'(t)$$

And:

$$\frac{\partial^2 V}{\partial r^2} = C(t)\cdot R''(r)$$

Then we have:

$$C(t)\cdot R''(t) = \frac{1}{D}\cdot R(r)\cdot C'(t)$$

It can be rearranged into:

$$\frac{R''(r)}{R(r)} = \frac{1}{D}\cdot\frac{C'(t)}{C(t)}$$

Since the left side is only be r-dependent and the right side is only be t-dependent, and since they equal to each other, they must be neither r- or t- dependent. So, we have:

$$\frac{R''(r)}{R(r)} = \frac{1}{D}\cdot\frac{C'(t)}{C(t)} = -\lambda$$

Then we have:

$$R'' + \lambda R = 0$$

And

$$C' + \lambda DC = 0$$

From the above equation, we have:

$$\frac{dC}{dt} = -\lambda DC$$

$$\frac{dC}{C} = -\lambda D\cdot dt$$

$$\int_0^C \frac{dC}{C} = -\lambda D\cdot\int_0^t dt$$

$$lnC(t) - lnC(0) = -\lambda Dt$$

$$C(t) = e^{-\lambda Dt}\cdot C(0)$$

For

$$R'' + \lambda R = 0$$

$$\frac{d^2R(r)}{dr^2} = -\lambda\cdot R(r)$$

$$R(r) = \mathrm{A}\cos\sqrt{\lambda}\cdot r + \mathrm{B}\sin\sqrt{\lambda}\cdot r$$

Now we have:

$$V(r,t) = \sum_{\lambda}\left[\left(\mathrm{A}\cos\sqrt{\lambda}\cdot r + \mathrm{B}\sin\sqrt{\lambda}\cdot r\right)\cdot e^{-\lambda Dt}\right]$$

$$C(r,t) = \sum_{\lambda}\left[\left(\mathrm{A}\cos\sqrt{\lambda}\cdot r + \mathrm{B}\sin\sqrt{\lambda}\cdot r\right)\cdot\frac{e^{-\lambda Dt}}{r}\right]$$

When brining food, which involves soaking a low-concentration food sample (C0) in a high-concentration bath (Ch), the following boundary conditions apply:

For 0 ≤ r ≤ R, where R is the radius of the spherical food sample, the initial concentration distribution within the food is given by C(r,0) = C0.

For r ≥ R and any time t, the concentration of salt in the surrounding bath is maintained at C(r,t) = Ch.

We have:

$$A = 0, and\ \lambda = \left(\frac{n\pi}{R}\right)^2 \text{ where } n = 1, 2, 3, \ldots$$

We then have:

$$C(r,t) = C_h - \frac{2R(C_h - C_0)}{\pi \cdot r}\sum_{n=1}^{\infty}\left[\frac{(-1)^{n+1}}{n}\sin\frac{n\pi r}{R}\cdot e^{-Dn^2\pi^2 t/R^2}\right]$$

for ($0 \le r \le R$)

We define

$\tau = \frac{R^2}{\pi^2 \cdot D}$ as the time constant.

Thus, we have:

$$C(r,t) = C_h - \frac{2R(C_h - C_0)}{\pi \cdot r}\sum_{n=1}^{\infty}\left[\frac{(-1)^{n+1}}{n}\sin\frac{n\pi r}{R}\cdot e^{-n^2 t/\tau}\right]$$

The concentration at the center of the sphere is (r = 0):

$$C_c = C_h - 2(C_h - C_0)\sum_{n=1}^{\infty}\left[(-1)^{n+1}\cdot e^{-n^2 t/\tau}\right]$$

We can spell out the equation with some of the initial (and deciding) terms:

$$C_c = C_h - 2(C_h - C_0)\{e^{-t/\tau} - e^{-4t/\tau} + e^{-9t/\tau} - e^{-16t/\tau} + e^{-25t/\tau} - e^{-36t/\tau} + e^{-49t/\tau} - \ldots\}$$

Where: $\tau = \frac{R^2}{\pi^2 \cdot D}$